Road profile estimation using an adaptive Youla- Kučera parametric observer: comparison to real profilers

Moustapha Doumiati, John Jairo Martinez Molina, Olivier Sename, Luc Dugard, Daniel Lechner

Road profile estimation using an adaptive Youla-Kučera parametric observer: comparison to real profilers

M. Doumiati [*] **O. Sename** [**] **J. Martinez** [**] **L. Dugard** [**]
D. Lechner [***]

[*] *ESEO Group, High School of Engineering, Electronics and Control Department, 10 Bd Jean Jeanneteau, 49100 Angers, France (email: moustapha.doumiati@eseo.fr)*
[**] *Univ. Grenoble Alpes, GIPSA-Lab, F-38000 Grenoble, France (email: olivier.sename@gipsa-lab.grenoble-inp.fr).*
[***] *IFSTARR Laboratory, MA Department, 13300 Salon de Provence, France (email: daniel.lechner@ifsttar.fr)*

Abstract: Road profile acts as a disturbance input to the vehicle dynamics and results in undesirable vibrations affecting the vehicle stability. A precise information of this data is mandatory for a better understanding of the vehicle dynamics behavior and active vehicle control systems design. However, direct measurements of the road profile are not trivial for technical and economical reasons, and thus alternative solutions are needed. This paper develops a novel observer, known as virtual sensor, suitable for real-time estimation of the road profile. The developed approach is carried on a quarter-car model and on measurements of the vehicle body. The road elevation is modeled as a sinusoidal disturbance signal acting on the vehicle system. Since this signal has unknown and time-varying characteristics, the proposed estimation method implements an adaptive control scheme based on the internal model principle and on the use of Youla-Kučera (YK) parametrization technique (also known as Q-parametrization). For performances assessment, estimations are comparatively evaluated with respect to measurements issued from Longitudinal Profile Analyzer (LPA) and Inertial Profiler (IP) instruments during experimental trials. The proposed method is also compared to the approach provided in (Doumiati et al. (2011)), where a stochastic Kalman filter is applied assuming a linear road model. Results show the effectiveness and pertinence of the present observation scheme.

Keywords: Road profile; Youla-Kučera parametrization; Vehicle dynamics; Profilers.

1. INTRODUCTION

1.1 Motivation

Road geometries, irregularities and deformations constantly modify the vehicle positions and wheel orientations. Thus, road profile is one of the most important factors that determines the vehicle performance. Its knowledge is essential for road quality evaluation, road roughness index calculation, vehicle dynamics analysis, suspensions design, and active control systems development (see (Gillespie (1992)), (Sayers and Karamihas (1998)), (Bastow et al. (2004)), (Elmadany and Abduljabbar (1999)), and (Savaresi et al. (2010))). For car manufacturers, road profile on-board evaluation would help to adjust the vehicle dynamics to improve passengers safety, ride comfort, and road holding through an *electronic stability program*. However, nowadays, there are no low-cost sensors that directly measure the road elevation. This motivates the development of an observer, also known as virtual sensor, to online reconstruct this data.

1.2 Paper contribution vs. State of arts

Road profile evaluation is a complex task. For experimental purposes, tools called profilers, profilometers or profilographs are usually employed to take measurements of the road profile. However, cost and installation constraints degrade the applicability of these instruments in ordinary vehicles (see Section 2). Other profile measurement methods are based on visual inspections as in (Kim et al. (2002)). Recently, Mercedes-Benz introduces in its new 2014 S- and E-Class cars stereo cameras for road profile scanning (Mercedes-Benz (2014)). These sensing techniques are extremely expensive and require some specialized operations, i.e sensibility to sensors location, hard signal processing, and so on. Moreover, the application of laser sensors for profile measurement is impractical in rainy weather. As an alternative, research involving use of observers for road profile estimation has gained prominence. In (Yousefzadeh et al. (2010)), an artificial nonlinear neural network (ANN) based approach was adopted to estimate the random road excitation. Authors employed a seven acceleration measurements vector as input for the estimation process where the road profile is modeled as a function of the road roughness coefficient. For a good classification, the vehicle behavior under different standardized roads (ISO 8608) must be incorporated in the (ANN) learning phase. Similarly, authors in (Solhmirzaei et al. (2012)) proposed a solution for road profile estimation using multi-input multi-output feed forward wavelet neural network (WNN). A novel approach based on the cross-entropy method employing Monte Carlo techniques was given in (Harris et al. (2010)) to obtain road profile estimation using the sprung and unsprung mass accelerations. The proposed ANN, WNN, and Monte-Carlo estimators require too much computing time, and could be practically impossible to be implemented on real-time applications.

In (Imine et al. (2005)) and (Imine et al. (2006)), estimation techniques based on model-based sliding mode observers were proposed. Therein, authors considered a full car model of 16 Degree Of Freedom (DOF). Such a complex vehicle model appears time-consuming for on-board implementation. Recently, in (Rath et al. (2014)), authors developed a road profile estimator using adaptive super-twisting theory and considering nonlinear dynamics of the spring and damper of an active suspension system. In (Tudón-Martinez et al. (2014)), an $\mathcal{H}_\infty$ robust observer was used to estimate the variables monitoring the suspension dynamics from accessible vehicle measurements. The estimated variables were then used in the static equation of the unsprung mass acceleration to calculate the road excitation. In (Doumiati et al. (2011)), authors proposed a method based on an augmented quarter of vehicle (QoV) state-space model, where the road profile and its velocity were incorporated as unknown states. The observation process was built on a recursive Kalman estimator for on-board applications. The studies in (Doumiati et al. (2011)), (Imine et al. (2005)) and (Imine et al. (2006)) assumed linear road profile models neglecting profile accelerations. However, this hypothesis does not fully satisfy the analysis of the road profile presented in (Sayers and Karamihas (1998)). Therein, a demonstration was given that even small road profile variations could lead to considerable road accelerations depending on the current vehicle velocity.

According to the road roughness classification ISO 8608 discussed in (Gonzáles et al. (2008)), a real road profile could be interpreted and evaluated by means of its spectral decomposition. A typical road profile has no direct resemblance to a pure sinusoid, but it encompasses a spectrum of sinusoidal wave lengths. This hypothesis is adopted in this study, and constitutes one of its particularity with respect to others existing in literature. The proposed procedure in this paper considers the road profile as unpredictable and random input disturbance to the vehicle system. Since this sinusoidal disturbance has unknown and time-varying amplitudes and frequencies, the estimation problem is tackled in the feedback adaptive control context applying the internal model principle (introducing the disturbance model into the controller) (refer to (Ioannou and Sun (1996)) and (Landau et al. (2011))). The given estimation process is a real-time conditioning algorithm. It is formulated as a closed-loop regulation approach, trying to attenuate the difference between the measured chassis position and the QoV model output. To simplify the design and reduce the computation load, the developed controller is built within the Youla-Kučera (YK) parametrization framework. The work given here is an extension of the study reported by the present authors in (Doumiati et al. (2014)). Note that in (Tudón-Martinez et al. (2015)), a part of the present authors used YK principle and online Fourier transform analysis for road roughness classification. The main contributions of this study with respect to (Doumiati et al. (2014)) and (Tudón-Martinez et al. (2015)) are:

- detailed synthesis of the observation scheme;
- experimental validation using different real profilers.

The rest of the paper is organized as follows. Section 2 describes some real profilers used for validation of the proposed method. Section 3 discusses the adopted vehicle and road models. Section 4 deals with the estimation process and discusses the observer design in a control scheme. Section 5 compares the estimation results to measured profiles during experimental tests. Finally, Section 6 provides concluding remarks and some perspectives for future works.

2. SOME EXISTING PROFILERS

Profilers or profilometers are instruments and methods used to produce a sequence of numbers related to the true road profile (Sayers and Karamihas (1998)). A profiler works by combining three main ingredients: a reference elevation, a height relative to the reference, and the longitudinal distance. These ingredients are combined in different ways, based on the design of the profiler. Among the different existing profilers, this study considers the Longitudinal Profile Analyzer (LPA) and the Inertial Profiler (IP).

- The LPA illustrated in Figure 1 is an instrument developed by the French Roads and Bridges Central Laboratory (IFSTTAR laboratory previously named LCPC) (Imine et al. (2006, 2005)). It has been the subject of many studies and research. The system includes one or two single wheel trailers towed at constant speed by a car, and employs a data acquisition system. A ballasted chassis supports an oscillating beam holding a feeler wheel that is kept in permanent contact with the pavement by a suspension and damping system. The chassis is linked to the towing vehicle by a universal-jointed hitch. Vertical movements of the wheel result in angular travel of the oscillated beam, measured with respect to the horizontal arm of the inertial pendulum, independently of movements of the towing vehicle. The measurements are made by an angular displacement transducer associated with the pendulum. The induced electrical signals are amplified and then recorded. Rough measurements have to be processed to obtain a reliable measurement of the road profile (phase distortion correction). Although this device has proved to provide precise profile elevation measurements, it cannot be integrated in ordinary cars for technical reasons.
- The IP was basically introduced by the General Motors research laboratory in 1964 (Sprangler and Kelly (1964)). This technique uses accelerometers placed on the body of the measuring vehicle to establish an inertial reference. The recorded profile is independent of the type of the vehicle survey and of the profiling speed. The inertial reference serves to correct for the

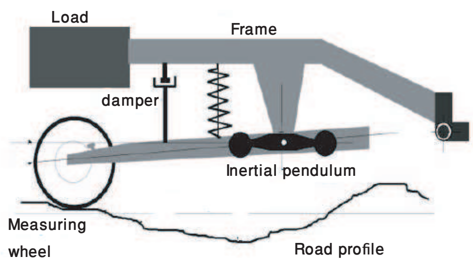

Fig. 1. *LPA*: Longitudinal Profile Analyzer (Imine et al. (2006)).

bounce of the survey vehicle. It is obtained using accelerometers placed on the body of the measuring vehicle. The vertical body motion (inertial reference) is obtained by double integration of the accelerometer signal. The relative displacement between the accelerometers and the pavement surface is measured with a non-contact light sensor mounted with the accelerometer on the vehicle body. Adequate filters must be used to eliminate noises in the acceleration signal and to suppress other distorted signal components due to the integration process. The elevation profile of the road is then obtained by subtracting the height sensor output from the absolute motion of the vehicle body (Imine et al. (2005, 2006)). The disadvantages of this method are its complete dependency on sensors location, weather conditions, and environment noises.

In the following, the performance of the proposed observer is compared to the LPA and IP tools.

3. MODELS OF THE VEHICLE/ROAD INTERACTIONS

To implement a model-based observer, suitable vehicle and road models must be assumed. The adopted models in this study are discussed in the next.

3.1 QoV vehicle model

For simplicity reasons, a linear passive QoV model (without actuation) that captures the most basic features of the vertical behavior of the vehicle is considered. This model represents a corner of a vehicle as shown in Figure 2. It accounts for about 75% of the vertical vibrations present on a vehicle (Sayers and Karamihas (1998)). The suspension system joins chassis and tire. The sprung mass of the car body, m_s, is connected by a spring and damper to the unsprung mass, m_u, of the suspension components by the suspension spring, k_s, and the damper, c_s. The spring is considered linear because around 95% of its operating zone in an automotive application is linear. The tire is linked with the road displacement, $u(t)$, involving the tire's stiffness, k_t. It is assumed that the tire damping is negligible. A sensitivity analysis of k_s, c_s, k_u, and k_t parameters on the suspension performance was drawn in (Rajamani (2006)).

An analysis of the full car model and half car model responses to road irregularities given in (Rajamani (2006)) indicated that the suspensions can be designed independently at each wheel. The quarter car suspension model is

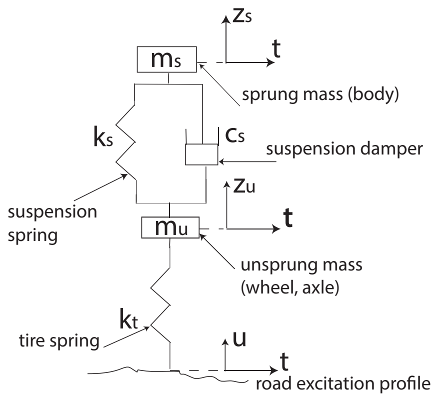

Fig. 2. QoV model.

therefore adequate to study and design automotive suspension systems for optimizing response to road irregularities. Assuming that wheels are rolling without slip and without contact loss, relations (1) and (2) represent the motion of the vehicle body and the wheel respectively:

$$m_s\ddot{z}_s = -k_s z_s - c_s\dot{z}_s + k_s z_u + c_s\dot{z}_u, \quad (1)$$

$$m_u\ddot{z}_u = -(k_s + k_t)z_u - c_s\dot{z}_u + k_s z_s + c_s\dot{z}_s + k_t u, \quad (2)$$

where $z_s(t)$ is the position of the vehicle body, $z_u(t)$ is the position of the wheel, and the *dot* denotes the time derivative, i.e., $\ddot{z}_s = \frac{d^2 z_s}{dt^2}$. In the *Laplace-domain*, the transfer function between the road profile $U(s)$ and the chassis position $Z_s(s)$, known as the road-to-body transmissibility equation, is of fourth-order and can be given by (3):

$$\frac{Z_s(s)}{U(s)} = \frac{a_1}{b_1 \cdot b_2 - b_3}, \quad (3)$$

where: $a_1 = k_t\,(sc_s + k_s)$, $b_1 = \left(s^2 m_s + sc_s + k_s\right)$, $b_2 = \left(s^2 m_u + sc_s + k_s + k_t\right)$, $b_3 = (sc_s + k_s)^2$.

The suspension system is designed so that it absorbs the road inputs, isolating the body from the road at high frequency road excitation ($> 1\ Hz$). At very low frequencies ($< 1\ Hz$), the vehicle body moves up and down almost exactly as does the ground. At about 1 Hz the body resonates on the suspension, amplifying the input from the road (Sayers and Karamihas (1998)).

3.2 Sinusoidal road profile model

The model of the road profile should be representative for a good estimation quality. Besides, it should be convenient for integration as input disturbance to the proposed observer formulated as a closed-loop regulation scheme.

As the vehicle moves over the road profile at a speed v, the static spatial waves (irregularities) of the road are transformed into *time-variant* sinusoidal elevation $u(t)$ at the wheel. The relation between the spatial wavelength, λ (respectively the wave number $\gamma = \frac{1}{\lambda}$) imposed by a part of the road profile and the resulting oscillation frequency, f, of the corresponding elevation signal is given by (Sayers and Karamihas (1998)):

$$f = \frac{v}{\lambda} = v.\gamma. \quad (4)$$

It could be observed that the travel speed affects how the vehicle sees sinusoidal waves in the road. More precisely,

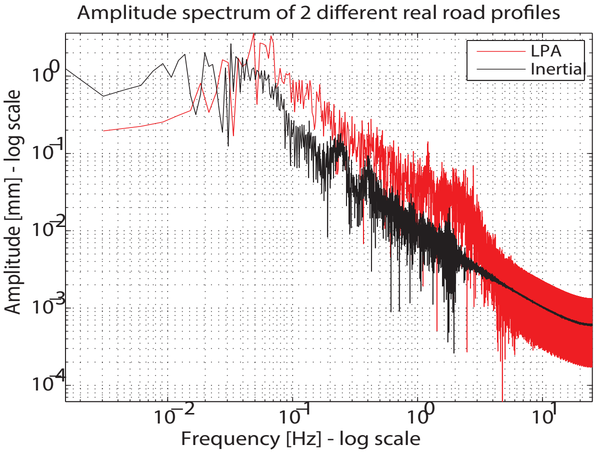

Fig. 3. Examples of spectra of two real road profiles.

according to ISO 8608, a typical road profile is a stochastic signal that has no direct resemblance to a pure sinusoid, but considered as a composition of series of sinusoidal waves (see (Rajamani (2006)), and (Sayers and Karamihas (1998))). Figure 3 shows examples of spectra of two different real road profiles collected through the LPA and IP instruments. These measurements are obtained using two laboratory cars moving at 75 Km/h and 25 Km/h respectively. The spectra of these low-pass signals are computed using the Fast Fourier transform.

Working hypothesis: Based on ISO 8608 classification, this study assumes that the time-based dynamics of the road profile can be modeled as a finite series of N sinusoids with different wavelengths, λ_i, frequencies, f_i, amplitudes, C_i, and phases, ϕ_i:

$$u(t) = \sum_{i=1}^{N} C_i sin(2\pi f_i t + \phi_i). \tag{5}$$

C_i, f_i, and ϕ_i are unknown time-varying parameters. There are no feasible prior information of these parameters that depend on: 1) suspension capability; 2) road surface (number of waveforms); 3) tire dynamics; and 4) vehicle velocity (Tudón-Martinez et al. (2015)). The objective of this paper is not to evaluate these parameters separately, but to estimate the road elevation $u(t)$.

4. OBSERVER DESIGN

4.1 Problem formulation

The estimation process developed in this study is formulated as a closed-loop regulation approach, trying to attenuate the difference e between the measured chassis position z_s and the estimated QoV model output $\hat{z}_s$ (see Figure 4). The chassis position signal is the result of the road profile disturbance input u on the vehicle system. A linear relation is assumed between z_s and u. The signal u is modeled as a time-varying (in frequency and amplitude) sinusoidal disturbance. When the estimated chassis position coincides with the corresponding measured one, so will also the estimated profile $\hat{u}$ be equivalent to u. In other terms, the command $\hat{u}$ could be interpreted as the estimated road profile required to produce $\hat{z}_s$, so that $e = z_s - \hat{z}_s = 0$. The problem becomes to find a control law for unknown time-varying disturbances rejection, case where the plant model (vehicle system) is known, and the disturbance model (road) is of unknown parameters.

One of the approaches considered for solving this problem is to build/estimate the disturbance model, and then recompute the controller in real-time. This leads to indirect adaptive control (Landau and Airimitoaie (2013)). The time-consuming part of this approach is the redesign of the controller at each sampling time. This method seems not to be practical for the present application due to the fast dynamics of the unpredicted variations of the road profile. Another way, known as direct adaptive control, consists to apply YK parametrization of the controller also known as Q-parametrization, where it is possible to insert and adjust the internal model (model of the disturbance) in the controller by adjusting the parameters of the Q-polynomial without recomputing the whole controller (polynomials R_0 and S_0 remain unchanged, see Figure 5). YK parametrization technique reduces the computation load and enhances the controller performances. Authors in (Constantinescu et al. (2007)) and (Landau and Airimitoaie (2013)) proved that the direct adaptive control scheme has simpler structure, implementation, and provides better performance than an indirect adaptive control scheme, especially during transient dynamic phases. Based on the analysis given above, it is recommended to develop the road profile observer in the direct adaptive control framework.

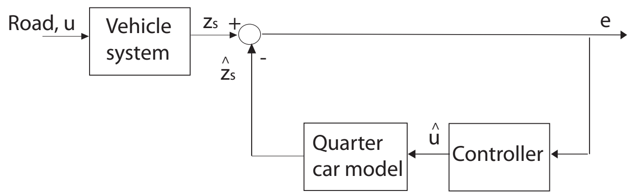

Fig. 4. Problem formulation: block diagram of the observer interpreted as a closed-loop control system.

4.2 Observability

Because the road profile is deduced from the vehicle measurements, the observability condition must be ensured. In (Doumiati et al. (2011)), it was verified that the sprung mass position offers sufficient information leading to a fully observable QoV model. Moreover, the *Gilbert observability criterion* assures full observability even if the road disturbance model is represented by a sum of sinusoidal waves (Tudón-Martinez et al. (2015)).

On a real vehicle, the sprung mass position z_s on a corner of the vehicle can be computed using an accelerometer and a suspension deflection sensor. As z_s is function of the vehicle load, mass uncertainties, and load distribution, an online estimator of the sprung mass is required (Yu et al. (2013)).

4.3 Direct adaptive control scheme

The discrete (digital) direct adaptive control scheme for time-varying disturbance rejection could be illustrated as in Figure 5. It uses YK parametrization for the computation of the controller. This algorithm takes its root from the idea of Tsypkin (Tsypkin (1991)). The common framework is the assumption that the disturbance is the result of a white noise or a Dirac impulse passed through the "model of disturbance (road)" considered unknown. The polynomials $A(z^{-1})$ and $B(z^{-1})$ obtained using the Z-transform of Equation (3), represent the denominator and the numerator of the dynamic car model.

The adaptive controller to be built is of RS-type. Its dynamic is separated into a nominal part (also called central controller), defined by $[R_0(z^{-1}), S_0(z^{-1})]$, and a performing part given by the polynomial $\hat{Q}$ that includes the disturbance model ($\hat{Q}$ denotes the estimation of the Q polynomial required to suppress disturbances). The controller $[R_0(z^{-1}), S_0(z^{-1})]$ is built so that it stabilizes the closed-loop system, and verifies desired specifications in the absence of the disturbance (without internal model of the disturbance, $\hat{Q} = 0$). It can be computed using classical methods in control theory, i.e pole placement method. Once calculated, (R_0, S_0) remains unchanged in the control scheme, but $\hat{Q}$ is adjusted online according to an adaptive algorithm to make $e(t) = 0$ in the presence of disturbances without modifying the closed-loop poles (Landau et al. (2005)). The controller $[R(z^{-1}), S(z^{-1})]$ transfer function is given by :

$$\frac{R(z^{-1})}{S(z^{-1})} = \frac{R_0(z^{-1}) + A(z^{-1})Q(z^{-1})}{S_0(z^{-1}) - B(z^{-1})Q(z^{-1})}. \tag{6}$$

The Q-parametrization offers a supplementary degree of freedom into the controller permitting to treat separately the problem of disturbances suppression. For details, robustness and stability analysis of the YK parametrization in the framework of adaptive control, one can refer to (Ioannou and Sun (1996)), (Landau et al. (2005)), and (Landau et al. (2011)). This study is only restricted to a brief presentation of the adaptive algorithm and the online calculation of the polynomial $\hat{Q}$.

The order n_Q of the polynomial Q is fixed, and depends upon the structure of the road wavelengths. According to (Tudón-Martinez et al. (2015)) two coefficients in the $\hat{Q}$ vector are enough to characterize the frequency of one unknown sinusoidal disturbance.

Let q^{-1} be the delay operator used for describing the system behavior in the time domain (i.e $x(t) = q^{-1}x(t+1)$). The operator z^{-1} is applied for representation in the frequency domain. Using the Q-parametrization, the output of the system in the presence of disturbance can be written as:

$$e(t) = \frac{S_0(q^{-1}) - B(q^{-1})Q(q^{-1})}{P(q^{-1})} w(t), \tag{7}$$

where $P(q^{-1})$ represents the poles of the closed loop:

$$P(q^{-1}) = A(q^{-1})S_0(q^{-1}) + B(q^{-1})R_0(q^{-1}), \tag{8}$$

and $w(t)$ (see Figure 5) is:

$$w(t) = A(q^{-1})e(t) + B(q^{-1})\hat{u}(t). \tag{9}$$

In the time domain, the internal model principle could be explained as find Q such that $e(t)$ becomes asymptotically zero.

Define $\hat{Q}(t, q^{-1})$ the estimation of the polynomial Q at instant t:

$$\hat{Q}(t, q^{-1}) = \hat{q}_0(t) + \hat{q}_1(t)q^{-1} + \cdots + \hat{q}_{n_Q}(t)q^{-n_Q}, \tag{10}$$

the associated estimated parameter vector:

$$\hat{\theta}(t) = [\hat{q}_0(t)\ \hat{q}_1(t)\ \ldots\ \hat{q}_{n_Q}(t)]^T. \tag{11}$$

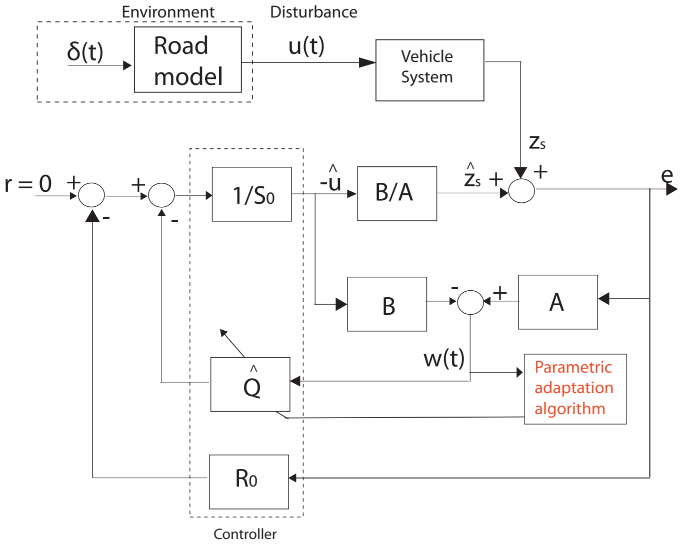

Fig. 5. Block diagram of the adaptive observer using the Q-parametrization: problem formulated as a closed-loop regulation control.

Define the following observation (regressor) vector:

$$\phi^T(t) = [w_2(t)\ w_2(t-1)\ \ldots\ w_2(t-n_Q)], \tag{12}$$

where:

$$w_2(t) = \frac{B^*(q^{-1})}{P(q^{-1})} w(t),\ B = q^{-1}B^*. \tag{13}$$

The *a priori* adaptation error, defined as the value of $e(t)$ obtained with $\hat{Q}(t, q^{-1})$, may be written as (details are provided in (Landau et al. (2009)), and (Landau et al. (2011)):

$$\epsilon^0(t+1) = w_1(t+1) - \hat{\theta}^T(t)\phi(t), \tag{14}$$

The *a posteriori* adaptation error (using $\hat{Q}(t+1, q^{-1})$), may be expressed as:

$$\epsilon(t+1) = w_1(t+1) - \hat{\theta}^T(t+1)\phi(t), \tag{15}$$

with

$$w_1(t+1) = \frac{S_0(q^{-1})}{P(q^{-1})} w(t+1), \tag{16}$$

$$w(t+1) = A(q^{-1})e(t+1) + B^*(q^{-1})\hat{u}(t), \tag{17}$$

where $B^*(q^{-1})\hat{u}(t) = B(q^{-1})\hat{u}(t+1)$.

For estimation of $\hat{Q}(t, q^{-1})$ parameters, the following Parameter Adaptation Algorithm (PAA) is used (Landau et al. (2005)):

$$\hat{\theta}(t+1) = \hat{\theta}(t) + F(t)\phi(t)\epsilon(t+1), \tag{18}$$

$$\epsilon(t+1) = \frac{\epsilon^0(t+1)}{1 + \phi^T(t)F(t)\phi(t)}, \tag{19}$$

$$\epsilon^0(t+1) = w_1(t+1) - \hat{\theta}^T(t)\phi(t), \tag{20}$$

$$F(t+1) = \frac{1}{\lambda_1(t)}(F(t) - \frac{F(t)\phi(t)\phi^T(t)F(t)}{\alpha(t) + \phi^T(t)F(t)\phi(t)}), \tag{21}$$

where $F(t)$ is a time-varying adaptation gain (positive definite matrix), and $\alpha(t) = \frac{\lambda_1(t)}{\lambda_2(t)}$. $F(t)$ can be interpreted as a measure of the parametric error. The tuning factors $\lambda_1(t)$ and $\lambda_2(t)$ permit the adjustment of the adaptation speed. At the beginning of the adaptation, the gain is high and then it decreases once the Q-parameter values are being adapted.

For *adaptive* operation, the following procedure works continuously and is applied sequentially at each sampling time:

(1) Get $e(t+1)$ and -$\hat{u}(t)$ to compute $w(t+1)$ using (17).
(2) Compute $w_1(t+1)$ and $w_2(t)$ through (13) to (16).
(3) Estimate the Q-polynomial using the parametric adaptation algorithm given by (18) to (21)
(4) Calculate $\hat{u}(t+1)$ according to:

$$S_0(q^{-1})\hat{u}(t+1) = R_0(q^{-1})e(t+1) + \hat{Q}(t, q^{-1})w(t+1). \quad (22)$$

4.4 Choice of the adaptation gain

To optimize the performances of the PAA, it is useful to tune the time profile of the adaptation gain $F(t)$ through two parameters: $\lambda_1(t)$ and $\lambda_2(t)$. An adaptation gain with a variable forgetting factor $\lambda_1(t)$ combined with a constant trace of $F(t)$ is chosen to track automatically the changes of the road characteristics. This adaptation regime is required for the case where no initial information is available upon the unknown parameters.

$F(t)$ with variable forgetting factor:
The variable forgetting factor is given by:

$$\lambda_1(t) = \lambda_0\lambda_1(t-1) + 1 - \lambda_0, \quad (23)$$

with $0 < \lambda_0 < 1$. λ_1 goes to 1 as $t \to +\infty$. A typical value of $\lambda_2(t)$ is 1. It is proved that for the variable forgetting factor λ_1, $F(t)$ asymptotically tends toward a decreasing adaptation gain (Landau et al. (2011)).

$F(t)$ with constant trace:
The trace is defined as the sum of the diagonal terms of the gain matrix $F(t)$. Constant trace means that:

$$tr(F(t)) = tr(F(t+1)) = tr(F(0)) = n_Q\xi, \quad (24)$$

where,

$$F(0) = diag(\xi...\xi), \ 0.01 < \xi < 4 \quad (25)$$

$$tr(F(t+1)) = \frac{1}{\lambda_1(t)} tr(F(t) - \frac{F(t)\phi(t)\phi^T(t)F(t)}{\alpha(t) + \phi^T(t)F(t)\phi(t)}). \quad (26)$$

In this case, one computes $\lambda_1(t)$ for $\alpha(t)$ fixed.

Finally, the PAA algorithm switches from the case of *variable forgetting factor* to the case of *constant trace* when $tr(F(t)) < n_Q\xi$.

5. EXPERIMENTAL RESULTS

In this section, the proposed YK parametric estimator is compared to the LPA and IP instruments through two experimental tests using two different lab cars. The signals coming from the profilers constitute the reference profiles. These data correspond to random sequences of road disturbances. They were collected during real trials, and then treated off-line. Figure 3 shows the spectra of the collected road profiles. In the following, the test scenarios, observer configurations, and results are illustrated and analyzed. A comparison of the present methodology with the Kalman based approach developed in (Doumiati et al. (2011)) is also provided in the next. For the following tests, vehicles are moving straightly, and their body positions are obtained by double integration of the signals generated by the accelerometers installed at the vehicles' corners in the vertical direction. Due to the fast up and downward movements, the vertical acceleration signals are noisy, and thus well calibrated band pass numerical filters are applied in the signals processing phase (Doumiati et al. (2011) and (Doumiati et al. (2013)).

5.1 Test 1 : comparison with (LPA) profiler

The experimental vehicle shown in Figure 6 is the LCPC Laboratory test vehicle. It is a Peugeot 406 equipped with accelerometers, relative suspension deflections sensor and towing *LPA* for road profile measurement. The suspension/tire parameters are: $m_s = 378\ Kg$, $c_s = 3000\ Ns/m$, $k_s = 21319\ N/m$, $m_u = 36.8\ Kg$, and $k_t = 100000 N/m$ (Imine et al. (2006)). Among numerous experimental tests, a trial made at the LCPC Laboratory test track is considered. The car runs on an irregular surface with a quasi-constant speed of 72 km/h along 600 m. The results illustrated in the following correspond to the left front wheel. Figure 7 shows the body positions in response to the road disturbance input.

Regarding the nominal controller (R_0, S_0) (without the internal model of the disturbance), it is designed via *MATLAB/SISO* tool so that it reconstructs the low frequencies part of the profile elevation. Figure 8 draws the output sensitivity function of the system defined as the transfer function between z_s and the output of the system e:

$$\frac{e}{z_s} = \frac{S_0A}{S_0A + R_0B}, \text{ where } \hat{Q} = 0. \quad (27)$$

The polynomials $R_0(z^{-1})$ and $S_0(z^{-1})$ are found to be:

$$R_0 = 9.15 - 16.6z^{-1} + 8.04z^{-2}, \ S_0 = 1 - z^{-1}. \quad (28)$$

The number of parameters in the Q-vector is experimentally obtained because the number and the characteristics of the waves that determine the road profile are unknown. Figure 9 displays the residual variance between u and $\hat{u}$ for different n_Q. The error reduction is negligible for $n_Q > 8$. Thus, eight parameters representing the sum of four sinusoidal waves seem enough to illustrate the road elevation of Test 1.

Figure 10 plots the estimated road profile via the proposed control approach and the one measured by the *LPA*. Clearly, the estimated values match well the LPA signal. However, some discrepancies in amplitudes persist. They might be caused by sensors calibration and filtration process in the LPA system. Figure 11 shows the variations of the polynomial $\hat{Q}$ coefficients. These coefficients are adapted as function of the involved road frequencies, and converge to some suitable values to ensure good estimations.

5.2 Test 2 : Comparison with Inertial profiler

In this test, the IFSTARR-MA laboratory vehicle (see Figure 12) moves on an irregular surface at a quasi-constant speed of 25 km/h. Some interesting parameters of the QoV model are given as: $m_s = 411\ Kg$, $c_s = 1146\ Ns/m$, $k_s = 20000\ N/m$, $m_u = 41\ Kg$, and $k_t = 100000\ N/m$. A bump is encountered on the roadway at almost 50 m from the departure point. The vehicle platform includes the required sensors and data acquisition system to run

Fig. 6. LCPC laboratory vehicle towing *LPA* (Imine et al. (2006)).

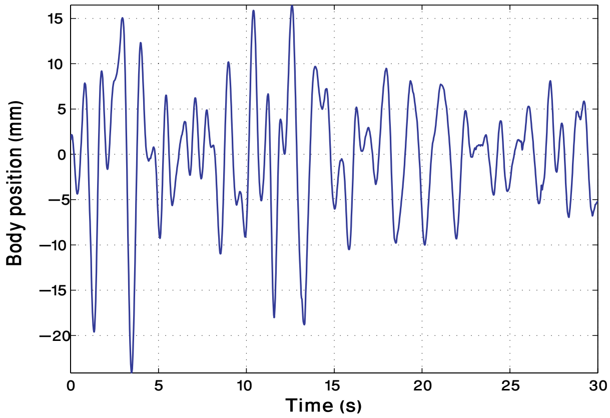

Fig. 7. Test 1: Up and downward vehicle body movements due to road irregularities.

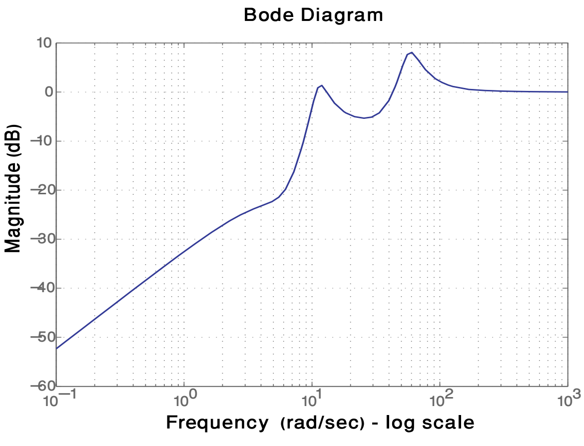

Fig. 8. Sensitivity function: $\frac{e}{z_s}$ for $\hat{Q} = 0$

the inertial profiling method. The distance between the vehicle body and the road is measured by a high-quality optical sensor.
The YK controller configuration is given as in the previous subsection. The calculated central controller using *Matlab/SISO* toolbox is found to be:

$$R_0 = 8.4 - 15.7z^{-1} + 7.5z^{-2}, \;\; S_0 = 1 - z^{-1}. \qquad (29)$$

Figure 13 illustrates the IP signal and the estimated profile on the rear right wheel. Once again, the obtained results

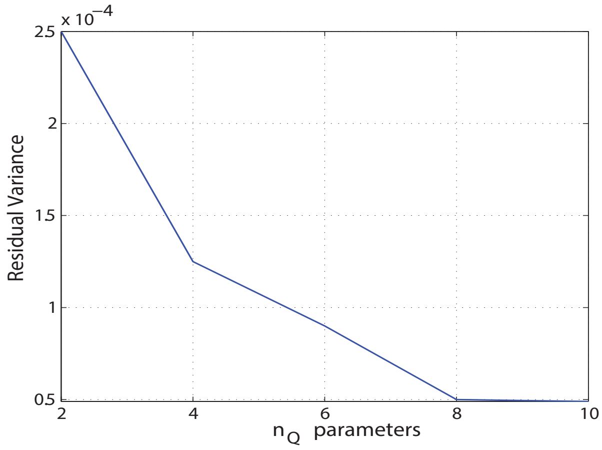

Fig. 9. Test 1: Sensitivity study on n_Q; Residual variance ($mm^2 \times 10^{-4}$) function of n_Q parameters.

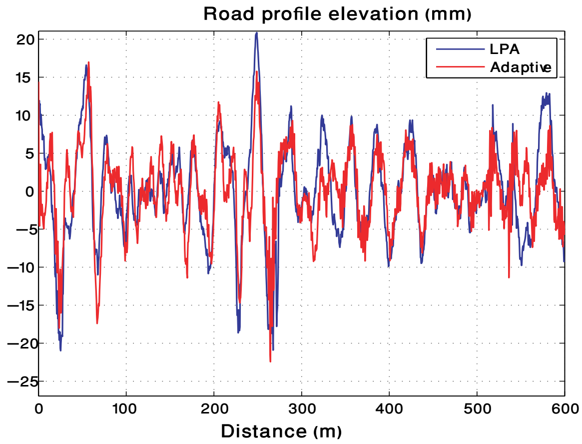

Fig. 10. Test 1: Comparison between the proposed adaptive observer approach and the LPA signal.

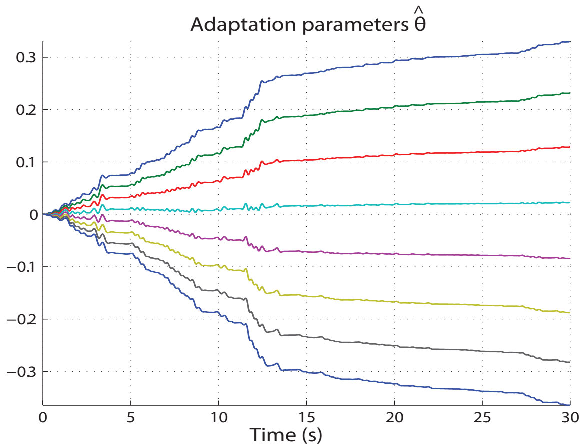

Fig. 11. Test 1: Evolution of $\hat{Q}$ parameters during online adaptation.

confirm the validation of the YK observer along the trial. Figure 14 gives the variation of the Q-polynomial coefficients. At the beginning, the parameters converge almost to the same value; then, all parameters are adapted again when the vehicle passes through the bump. Afterward, the parameter vector keeps almost constant values because the

Fig. 12. IFSTARR-MA laboratory car: Peugeot 307

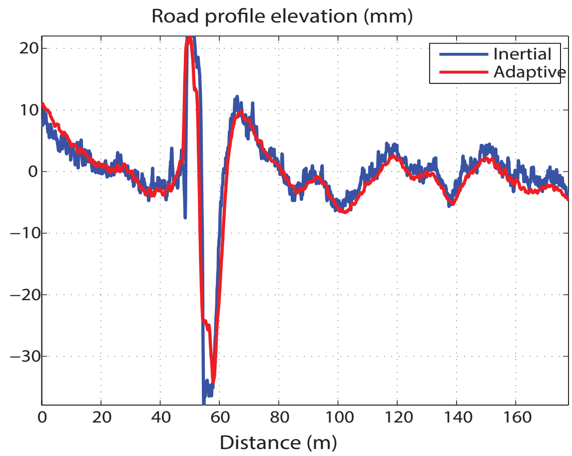

Fig. 13. Test 2: Comparison between the proposed adaptive observer approach and the Inertial profile.

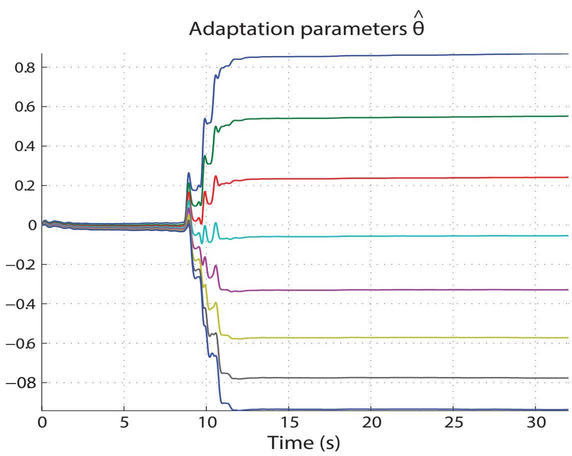

Fig. 14. Test 2: Evolution of $\hat{Q}$ parameters during online adaptation.

remaining part of the road is smoother than the previous part including the bump. Comparing Figures 11 and 14, it can be deduced that the Q-parameters in Test 2 are more dispersed than those identified in Test 1. This could be explained by the fact that the vehicle in Test 2 tackles a non homogenous road due to the occasional presence of a bump. Authors also believe that as the vehicle moves on rougher roads, higher Q- parameters values will be identified meaning that the controller is demanding more efforts to reject input disturbances, and so to achieve good estimation of the profile.

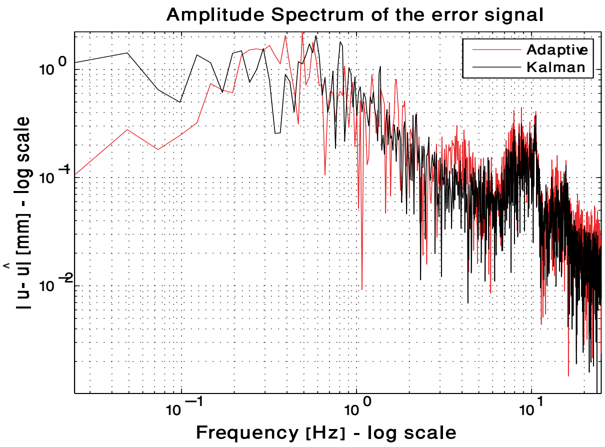

Fig. 15. Test 1: Spectrum of the estimation error signal, $u - \hat{u}$: comparison between the proposed adaptive approach and the Kalman observer.

5.3 Comparison with a Kalman based estimator

For more precise quantification of the estimation qualities, Figures 15 and 16 illustrate the spectra of the estimation errors for Test 1 and Test 2, respectively. It is deduced that the observer performs well especially for low frequencies corresponding to high wavelengths. These figures also compare the performance of the present method to the study given in (Doumiati et al. (2011)). Recall that the previous study assumed low road acceleration signal, $\ddot{u} = 0$, and applied a model-based stochastic Kalman filter for profile estimation. The road profile and its velocity were included in the states vector. Results prove that the proposed YK approach points out better performances especially for small frequencies that are crucial for suspension control. This is mainly due to the better representation and modeling of the road profile in the estimation process. Other advantages of the novel proposed method comparing to the Kalman one are:

- less costly method: since it requires only information regarding the body position, whilst the previous method needed measurements of the suspension deflections, the body position and acceleration.
- simpler tuning approach: since it only demands the regulation of the adaptation gain parameters, whilst the proposed Kalman method built on six states and three measurements required the regulation of a 6×6 and 3×3 noise variance-covariance matrices.

6. CONCLUSION

This paper described a new model-based estimation process suitable for real-time implementation to reconstruct the elevation of the road. According to ISO 8608, a road profile satisfies a periodic motion of one or more sinusoidal waveforms, whose fundamental frequencies are not straightforward to compute. To build the model-based observer, the vehicle was represented by a QoV model while the road surface was modeled by a finite number of sinusoidal waves with time-varying characteristics (in amplitude and frequency). Since the estimation quality strongly depended on the unknown frequencies of the road profile excitation, an adaptive observer scheme was

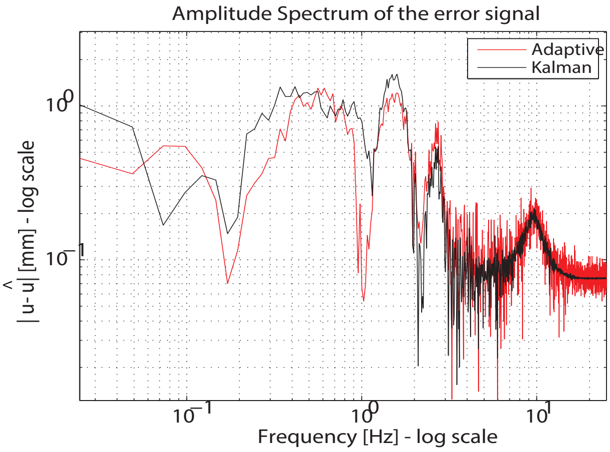

Fig. 16. Test 2: Spectrum of the estimation error signal, $u - \hat{u}$: comparison between the proposed adaptive approach and the Kalman observer.

designed by means of YK parametrization also known as Q-parametric observer. The road profile observation problem tackled in an adaptive control regulation scheme can be considered as a major contribution of this research. The profile reconstruction capacity was successfully tested through numerical simulations using experimental data issued from LPA and IP tools. The obtained results supported the validity and pertinence of the postulated working hypothesis and framework.

Further investigations consist to apply half or full-car vehicle model instead of a QoV model for a better representation of the vehicle dynamics in different driving situations (cornering, steering, accelerating, and braking). The proposed method will be also integrated in a global control scheme including semi-active suspensions among other actuators for vehicle stability and driving comfort.

ACKNOWLEDGEMENTS

Special thanks to the LCPC (www.ifsttar.fr) for the experimental data collected through their *LPA*. This real data was delivered in the framework of SARI/RADARR project in collaboration with Heudiasyc laboratory, France (www.hds.utc.fr).

REFERENCES

D. Bastow, G. Howard, and J. P. Whitehead. *Car suspension and handling*. SAE International, 2004.

A. Constantinescu, D. Rey, and I.D. Landau. Rejection of narrow band unknown disturbances in an active suspension system. In *Proceedings of the European Control Conference, Kos, Greece*, 2007.

M. Doumiati, A. Victorino, A. Charara, and D. Lechner. Estimation of road profile for vehicle dynamics motion: experimental validation. In *Proceedings of the American Control Conference, St Francisco, CA, USA*, pages 5237–5242, 2011.

M. Doumiati, A. Charara, A. Victorino, and D. Lechner. *Vehicle dynamics estimation using Kalman filtering - Experimental validation*. ISTE ltd and J. Wiley, 2013.

M. Doumiati, S. Erhart, J. Martinez, O. Sename, and L. Dugard. Adaptive control scheme for road profile estimation: application to vehicle dynamics. In *Proceedings of 19th IFAC World Congress, Cape, South Africa*, 2014.

M. M. Elmadany and Z. S. Abduljabbar. Linear quadratic gaussian control of a quarter-car suspension. *Vehicle System Dynamics*, 32:479–497, 1999.

T. D. Gillespie. *Fundamentals of vehicle dynamics*. Society of Automotive Engineers, 1992.

A. Gonzáles, E.J. O'Brien, Y.Y. Li, and K. Cashell. The use of vehicle acceleration measurements to estimate road roughness. *Vehicle System Dynamics*, 46:483–499, 2008.

N. K. Harris, A. Gonzáles, E. J. O'Brien, and P. McGetrick. Characterization of pavement profile heights using accelerometer readings and a combinatorial optimization technique. *Journal of Sound Vibrations*, 329(5): 497–508, 2010.

H. Imine, Y. Delanne, and N.K. M'sirdi. Road profile inputs for evaluation of the loads on the wheels. *Vehicle System Dynamics*, Supplement 43:359–369, 2005.

H. Imine, Y. Delanne, and N.K. M'sirdi. Road profile input estimation in vehicle dynamics simulation. *Vehicle System Dynamics*, 44(4):285–303, 2006.

P. A. Ioannou and J. Sun. *Robust adaptive control*. Prentice-Hall, 1996.

H. J. Kim, H. S. Yang, and Y. P. Park. Improving the vehicle performance with active suspension using road-sensing algorithm. *Computers and Structures*, 80(18-19):1569–1577, 2002.

I. Landau, A. Constantinescu, and D. Rey. Adaptive narrow band disturbance rejection applied to an active suspension-an internal model principle approach. *Automatica*, 41:563–574, 2005.

I.D. Landau and T. Airimitoaie. An indirect adaptive feedback attenuation strategy for active vibration control. In *Proceedings of the 21st Mediterranean Conference on Control and Automation, Chania, Greece*, 2013.

I.D. Landau, A. Constantinescu, and M. Alma. Adaptive regulation - rejection of unknown multiple narrow band disturbances. In *Proceedings of the 17th Mediterranean Conference on Control and Automation, Thessaloniki, Greece*, 2009.

I.D. Landau, R. Lozano, M. M'Saad, and A. Karimi. *Adaptive control: Algorithms, Analysis and Applications*. Springer-Verlag, 2011.

Mercedes-Benz, 2014. URL `http:www5.mercedes-benz.com`.

R. Rajamani. *Vehicle dynamics and control*. Springer, 2006.

J. J. Rath, K. C. Veluvolu, and M. Defoort. Estimation of road profile for suspension systems using adaptive super-twisting observer. In *Proceedings of 13th European Control Conference, Strasbourg, France*, 2014.

S. M. Savaresi, C. Poussot-vassal, C. Spelta, O. Sename, and L. Dugard. *Semi-active suspension control design for vehicles*. Elsevier, Butterworth Heinemann, 2010.

M. W. Sayers and S. M. Karamihas. *The little book of profiling*. University of Michigan, 1998.

A. Solhmirzaei, S. Azadi, and R. Kazemi. Road profile estimation using wavelet neural network and 7-dof vehicle dynamics model. *Journal of Mechanical Science and Technology*, 26(10):3029–3036, 2012.

E.B. Sprangler and W.J. Kelly. *Profilometer method for measuring road profile*. General Motors Research Publication GMR-452, 1964.

Y. Tsypkin. *Adaptive invariant discrete control systems*. Springer Verlag, 1991.

J. C. Tudón-Martinez, S. Fergani, O. Sename, R. Morales-Menendez, and L. Dugard. Online road profile estimation in automotive vehicles. In *Proceedings of 13th European Control Conference, Strasbourg, France*, 2014.

J. C. Tudón-Martinez, S. Fergani, O. Sename, J. J. Martinez, R. Morales-Menendez, and L. Dugard. Adaptive road profile estimation in semi-active car suspensions. *IEEE Transactions on Control Systems Technology, DOI 10.1109/TCST.2015.2413937*, 2015.

M. Yousefzadeh, S. Azadi, and A. Soltani. Road profile estimation using neural network algorithm. *Journal of Mechanical Science and Technology*, 24:743–754, 2010.

W. Yu, X. Zhang, K. Guo, H. R. Karimi, F. Ma, and F. Zheng. Adaptive real-time estimation on road disturbances properties considering load variation via vehicle vertical dynamics. *Mathematical Problems in Engineering*, Article ID 283528, 2013.